Discrete dislocation modelling of Nano- and Micro-indentation

Widjaja, Andreas

Chapter 3

Discrete dislocation plasticity

Abstract

This chapter provides a summary of the discrete dislocation plasticity model proposed by Van der Giessen and Needleman [1]. In this model a dislocation is treated as a line defect in a linear continuum media. Plasticity arises from the motion of dislocations on slip planes. Constitutive rules are also formulated for the nucleation from Frank-Read sources, dislocation annihilation, and dislocation pinning at obstacles.

The last section of this chapter presents the computational algorithm of the discrete dislocation dynamics simulation for the application to the indentation problem analysed in subsequent chapters.

3.1 Introduction

Indentation into a material causes elastic deformation initially, followed by plastic deformation if indentation is deep enough. Plastic deformation in crystalline metal arises from the collective motion of many dislocations. If indentation into the crystal is deep enough, which is the case for macro-indentation, the plastic zone is so large that plasticity can be modelled by a continuum description. For smaller sized plastic zones, such as during nanometer and micron size indentation, there are insufficient dislocations to be averaged out and they must be treated individually: discrete dislocation plasticity.

In discrete dislocation plasticity, an individual dislocation is treated as a line defect in a linear continuum. Plasticity is caused by the collective motion of many dislocations. A dislocation glides in response to a shear stress applied in a direction perpendicular to its line. Each dislocation I is characterised by its Burger's vector $\boldsymbol{b}^{(I)}$, gliding on its slip plane with direction unit vector $\boldsymbol{s}^{(I)}$ and normal $\boldsymbol{m}^{(I)}$.

The complete model comprises constitutive rules, governed by the internal stress state, which depends on the boundary conditions [1]. These rules connect the stress state with the dislocation structure evolution. Specifically, the constitutive rules control the ingredients of the model: dislocation glide on predefined slip planes, dislocation nucleation from Frank-Read sources, dislocation annihilation and dislocation pinning at obstacles.

3.2 General description of discrete dislocation plasticity

In this thesis, we use the versatile framework proposed by Van der Giessen and Needleman [1] to solve boundary value problems for dislocated bodies. Consider a finite body V containing a certain distribution of dislocations. The boundary $S = S_f \cup S_u$ of the body V is subject to traction or displacement boundary conditions: S_f and S_u are boundary portions where traction T_i^0 and displacement u_i^0 are prescribed, respectively. The traction is connected to the state of stress σ_{ij} via $T_i = \sigma_{ij} n_j$, where n_i denotes the unit outward normal to S.

The technique decomposes the problem into two parts: (i) the problem of interacting dislocations in the homogeneous infinite solid ($\tilde{(\ )}$-fields) and (ii) the problem of the nonhomogeneous body without dislocations ($\hat{(\ )}$-fields). This decomposition technique is illustrated in Fig. 3.1. Superposition of the two fields reads

$$u_i = \tilde{u}_i + \hat{u}_i \ , \qquad \epsilon_{ij} = \tilde{\epsilon}_{ij} + \hat{\epsilon}_{ij} \ , \qquad \sigma_{ij} = \tilde{\sigma}_{ij} + \hat{\sigma}_{ij} \ , \tag{3.1}$$

with the $\tilde{(\ )}$-fields for displacement, strain and stress contain contributions of all N

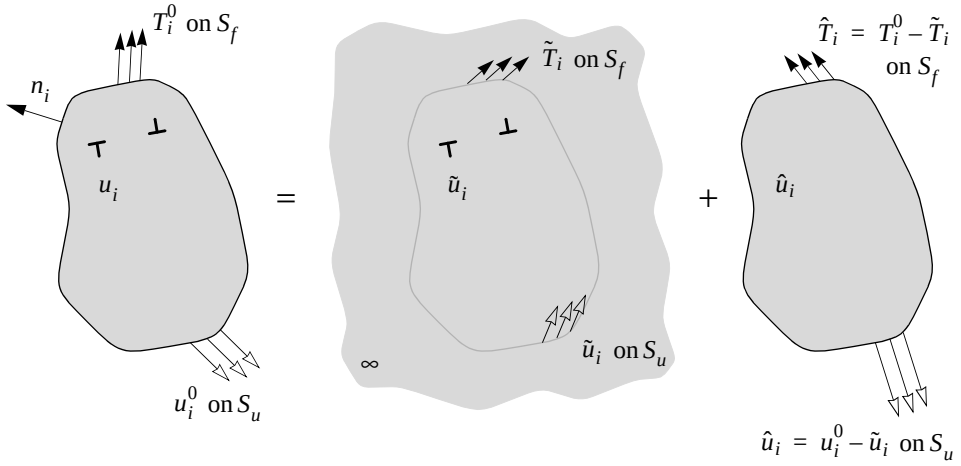

Figure 3.1 Decomposition of the problem for the dislocated body into the problem of interacting dislocations in the homogeneous infinite solid (the (˜)-fields) and the complementary problem for the body without dislocations (the (ˆ)-fields). This figure is reprinted with permission from [1].

individual dislocations,

$$\tilde{u}_i = \sum_{I=1}^{N} u_i^{(I)} \ , \qquad \tilde{\epsilon}_{ij} = \sum_{I=1}^{N} \epsilon_{ij}^{(I)} \ , \qquad \tilde{\sigma}_{ij} = \sum_{I=1}^{N} \sigma_{ij}^{(I)} \ , \tag{3.2}$$

and the (ˆ)-field is actually the smooth image field that corrects the boundary conditions on S. We solve the (ˆ)-field using finite element method.

The (ˆ)-fields are governed by the equilibrium condition

$$\frac{\partial \hat{\sigma}_{ij}}{\partial x_j} = 0, \tag{3.3}$$

or, equivalently through the principle of virtual work,

$$\int_V \hat{\sigma}_{ij} \delta \hat{\epsilon}_{ij} \ dV = \int_S \hat{t}_i \delta \hat{u}_i \ dA, \tag{3.4}$$

together with the strain-displacement relation

$$\hat{\epsilon}_{ij} = \frac{1}{2} \left(\frac{\partial \hat{u}_i}{\partial x_j} + \frac{\partial \hat{u}_j}{\partial x_i} \right), \tag{3.5}$$

and the constitutive relation

$$\hat{\sigma}_{ij} = L_{ijkl} \hat{\epsilon}_{kl}, \tag{3.6}$$

where L_{ijkl} are the elastic moduli. For isotropic elasticity,

$$L_{ijkl} = \frac{E}{1+\nu}\left[\frac{1}{2}(\delta_{ik}\delta_{jl} + \delta_{il}\delta_{jk}) + \frac{\nu}{1-2\nu}\delta_{ij}\delta_{kl}\right] \tag{3.7}$$

with E and ν being Young's modulus and Poisson's ratio, respectively.

The mixed traction-displacement boundary conditions read

$$\hat{T}_i = T_i^0 - \tilde{T}_i \qquad \text{on } S_f, \tag{3.8}$$

and

$$\hat{u}_i = u_i^0 - \tilde{u}_i \qquad \text{on } S_u. \tag{3.9}$$

The decomposition is fully three-dimensional. In this thesis, however, we will only deal with two-dimensional models of indentation. Under plane strain conditions perpendicular to the plane, all dislocations are of edge character.

3.3 Displacement and stress field of an edge dislocation

If the material is elastically isotropic, then the components $u_i^{(I)}$ $(i = 1, 2)$ of the infinite-body displacement field $\boldsymbol{u}^{(I)}$ at (x_1, x_2) due to a dislocation I with Burgers vector b positioned at $(X_1^{(I)}, X_2^{(I)})$ are given by the well-known expressions (see [2, 3])

$$u_1^{(I)}(x_i) = \frac{b}{2\pi(1-\nu)}\left[\frac{1}{2}\frac{\Delta x_1 \Delta x_2}{(\Delta x_1)^2 + (\Delta x_2)^2} - (1-\nu)\arctan\frac{\Delta x_1}{\Delta x_2}\right], \tag{3.10}$$

$$u_2^{(I)}(x_i) = \frac{b}{2\pi(1-\nu)}\left[\frac{1}{2}\frac{(\Delta x_2)^2}{(\Delta x_1)^2 + (\Delta x_2)^2} - \frac{1}{4}(1-2\nu)\ln\frac{(\Delta x_1)^2 + (\Delta x_2)^2}{b^2}\right], \tag{3.11}$$

where $\Delta x_i = x_i - X_i^{(I)},\ (i = 1, 2)$.

The components of the long-range stress field of this dislocation can be expressed as

$$\sigma_{11} = -\frac{Eb}{4\pi(1-\nu^2)}\frac{\Delta x_2\left[3(\Delta x_1)^2 + (\Delta x_2)^2\right]}{\left[(\Delta x_1)^2 + (\Delta x_2)^2\right]^2}, \tag{3.12a}$$

$$\sigma_{22} = \frac{Eb}{4\pi(1-\nu^2)}\frac{\Delta x_2\left[(\Delta x_1)^2 - (\Delta x_2)^2\right]}{\left[(\Delta x_1)^2 + (\Delta x_2)^2\right]^2}, \tag{3.12b}$$

$$\sigma_{12} = \frac{Eb}{4\pi(1-\nu^2)}\frac{\Delta x_1\left[(\Delta x_1)^2 - (\Delta x_2)^2\right]}{\left[(\Delta x_1)^2 + (\Delta x_2)^2\right]^2}, \tag{3.12c}$$

and are plotted in Fig. 3.2.

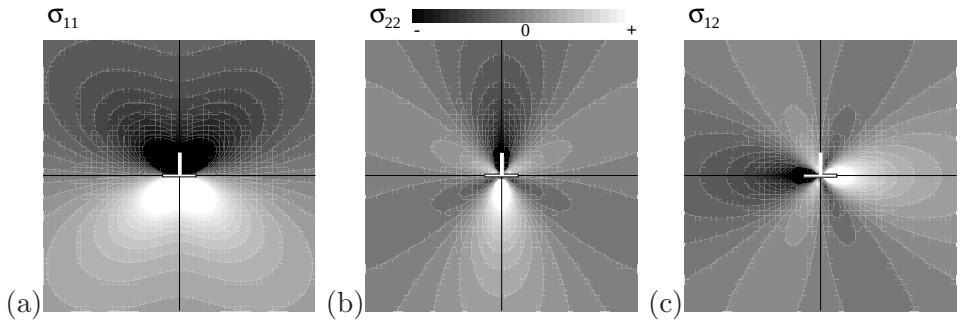

Figure 3.2 The (a) σ_{11}, (b) σ_{22}, and (c) σ_{12} components of the stress field of an edge dislocation.

3.4 The Peach-Koehler force and dislocation motion

The Peach-Koehler force $\boldsymbol{f}^{(I)}$ acting on the I-th dislocation is calculated from the stress state as

$$\boldsymbol{f}^{(I)} = \boldsymbol{t}^{(I)} \times \left[\left(\hat{\boldsymbol{\sigma}} + \sum_{J \neq I} \tilde{\boldsymbol{\sigma}}^{(J)} \right) \cdot \boldsymbol{b}^{(I)} \right], \tag{3.13}$$

where $\boldsymbol{t}^{(I)}$ and $\boldsymbol{m}^{(I)}$ are the unit tangent and slip plane normal vector to the dislocation I. The component of the Peach-Koehler force in the direction $\boldsymbol{t}^{(I)} \times \boldsymbol{m}^{(I)}$, *i.e.* in the slip plane and normal to the dislocation, is

$$f^{(I)} = \boldsymbol{m}^{(I)} \cdot \left(\hat{\boldsymbol{\sigma}} + \sum_{J \neq I} \tilde{\boldsymbol{\sigma}}^{(J)} \right) \cdot \boldsymbol{b}^{(I)}. \tag{3.14}$$

The motion of dislocation I follows Newton's second law of motion

$$m \frac{\mathrm{d}v^{(I)}}{\mathrm{d}t} = f^{(I)} - B v^{(I)}, \tag{3.15}$$

where m is the effective mass of the dislocation. The order of magnitude of m is the mass of the material contained within the dislocation core, $m \approx \rho b^2$ with ρ being the material density. As the associated inertia effects only play a role on picosecond time scales, while dislocation dynamics focuses on time scale of nanoseconds and larger, inertia effects can be safely neglected for quasi-static deformations. When a dislocation moves, it experiences a phonon drag directing opposite to its movement, with a drag coefficient B. When inertia is neglected, the Peach-Koehler force acting on the I-th dislocation causes it to move with velocity

$$v^{(I)} = \frac{f^{(I)}}{B}. \tag{3.16}$$

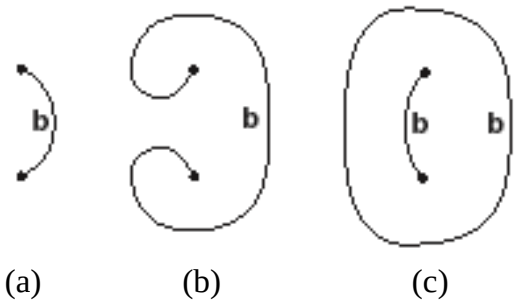

Figure 3.3 Illustration of the Frank-Read mechanism of dislocation nucleation (the sequence is shown from (a) to (c)): (a) Original pinned dislocation segment with Burger's vector $\boldsymbol{b}$. (b) The segment bows out and further (c) produce a new dislocation loop with Burger's vector $\boldsymbol{b}$, leaving a segment like it was initially.

In our calculations we take a fixed value of $B = 10^{-4}$ Pa s, which is representative for aluminium at room temperature.

3.5 Dislocation nucleation

Dislocations in a crystal can multiply. An important mechanism for this is the one proposed by two physicists W.T. Read and F.C. Frank [4]. The mechanism involves the bowing out of a dislocation pinned at two points, and the subsequent instability of the bowed dislocation which results in the formation of a dislocation loop and the retention of the original pinned dislocation.

The Frank-Read source is formed by a dislocation segment pinned at two points, see Fig. 3.3. A stress applied continuously to the pinned dislocation segment will cause the dislocation line to grow longer, but because the two ends are pinned, the curvature of the dislocation in the glide plane increases. Once the line exceeds a critical curvature, its movement becomes unstable and sweeps on outward without requiring further stress. Two segments of the curved line eventually touch and join to form a closed dislocation loop, thus leaving a short and new dislocation line segment between the original fixed end points. The newly formed dislocation loop is free to propagate on the glide plane.

For two-dimensional discrete dislocation plasticity, as used in the thesis, every Frank-Read segment is represented by a point source on a slip plane, and two nucleated edge dislocations (of opposite sign) represent the cross section of the newly generated loop. The mechanism is approximated as follows: If the resolved shear stress acting on the source exceeds a critical value τ_{nuc},

$$\tau \geq \tau_{\text{nuc}}, \tag{3.17}$$

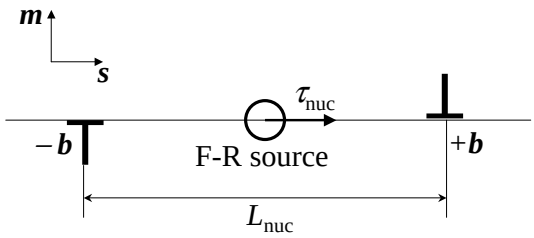

Figure 3.4 Schematic diagram of nucleation from a two-dimensional Frank-Read source. Two edge dislocations with opposite sign are nucleated with a distance L_{nuc} from each other, when the resolved shear stress exceeds the strength, τ_{nuc}, for a sufficiently long time.

for a sufficiently long time t,

$$t \geq t_{\mathrm{nuc}}, \tag{3.18}$$

two opposite edge dislocations (a dipole) are nucleated. The distance L_{nuc} between the dislocations, as shown schematically in Fig. 3.4, is taken as

$$L_{\mathrm{nuc}} = \frac{E}{2\pi(1-\nu^2)}\frac{b}{\tau_{\mathrm{nuc}}}, \tag{3.19}$$

so that τ_{nuc} exceeds (or at least, balances) the attractive shear stress that the dislocations exert one another.

3.6 Dislocation annihilation

When the stress so favours, it is possible that a dislocation loop collapses on itself and the defect disappears, leaving a perfect crystal. In two-dimensional discrete dislocation plasticity, the event is modelled by annihilating two opposite signed edge dislocations; when they meet each other within a distance L_{a} on the same slip plane. In this thesis $L_{\mathrm{a}} = 6b$ is used as the annihilation distance.

3.7 Dislocation obstacles

A moving dislocation can be stopped when it is hindered by an obstacle. In a heterogeneous plastically deforming material, precipitates, forest dislocations and grain boundaries can act as obstacles to the movement of a dislocation. In two-dimensions, obstacles are represented as fixed points assigned to a slip plane. A dislocation gliding on a slip plane can be stopped and pinned by an obstacle at the same slip plane. The pinned dislocation is released and free to move again only once the Peach-Koehler force on it is higher than b times the obstacle strength τ_{obs}.

Sometimes this happens to a pinned dislocation because a dislocation pile-up is formed behind it, which causes a very large force on it.

3.8 Algorithm of discrete dislocation dynamics

In this thesis, discrete dislocation plasticity is simulated using an incremental manner, adopting Euler time integration. In this incremental procedure, the stress and displacement fields are calculated at each time step, followed by updating the dislocation structure.

The general framework of discrete dislocation plasticity is used specifically in the indentation problem as the main topic of this thesis. The general algorithm of discrete dislocation dynamics, with specific application to indentation, is shown as a flow chart in Fig. 3.5.

References

[1] E. Van der Giessen and A. Needleman, Discrete dislocation plasticity: a simple planar model. *Modelling and Simulation in Materials Science and Engineering*, 3:689–735, 1995.

[2] F.R.N. Nabarro, *Theory of Crystal Dislocations*, Oxford: Oxford University Press, 1967.

[3] J.P. Hirth and J. Lothe, *Theory of Dislocations*, New York: McGraw-Hill, 1968.

[4] F.C. Frank and W.T. Read Jr., Multiplication Processes for slow moving dislocations. *Physical Review*, 79:722–723, 1950.

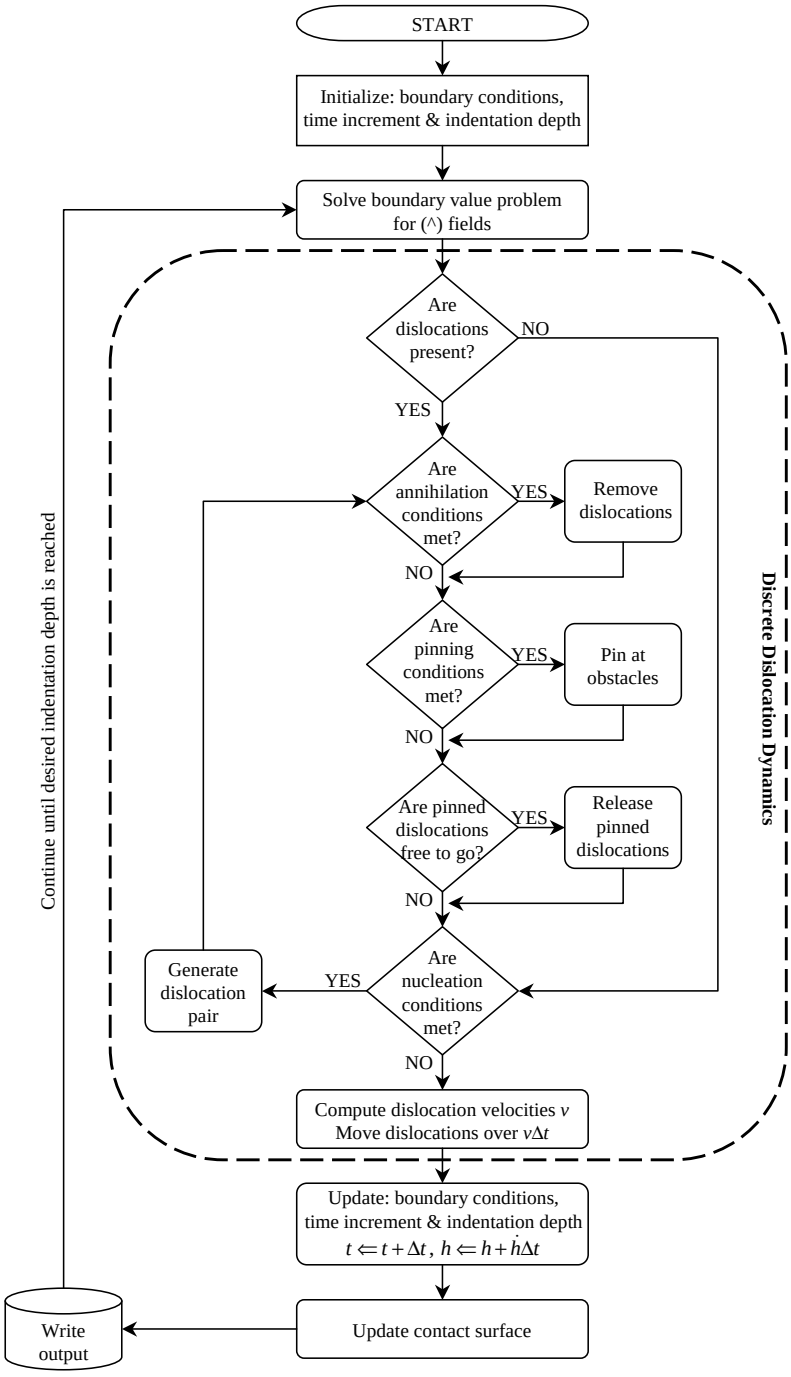

Figure 3.5 Flow chart of the computational algorithm of discrete dislocation based indentation. Discrete dislocation dynamics part is enclosed by a dashed line. The '⇐' operator denotes a variable assignment.